

Cessation of gastrulation is mediated by suppression of epithelial-mesenchymal transition at the ventral ectodermal ridge

journal or publication title	Development
volume	134
number	24
page range	4315-4324
year	2007-12
URL	http://hdl.handle.net/2298/10388

doi: 10.1242/dev.008151

Cessation of gastrulation is mediated by suppression of epithelial-mesenchymal transition at the ventral ectodermal ridge

Sho Ohta^{1,2}, Kentaro Suzuki¹, Katsuro Tachibana³, Hideaki Tanaka⁴ and Gen Yamada^{1,*}

In the gastrula stage embryo, the epiblast migrates toward the primitive streak and ingresses through the primitive groove. Subsequently, the ingressing epiblast cells undergo epithelial-mesenchymal transition (EMT) and differentiate into the definitive endoderm and mesoderm during gastrulation. However, the developmental mechanisms at the end of gastrulation have not yet been elucidated. Histological and genetic analyses of the ventral ectodermal ridge (VER), a derivative of the primitive streak, were performed using chick and mouse embryos. The analyses showed a continued cell movement resembling gastrulation associated with EMT during the early tailbud stage of both embryos. Such gastrulation-like cell movement was gradually attenuated by the absence of EMT during tail development. The kinetics of the expression pattern of *noggin* (*Nog*) and basal membrane degradation adjacent to the chick and the mouse VER indicated a correlation between the temporal and/or spatial expression of *Nog* and the presence of EMT in the VER. Furthermore, *Nog* overexpression suppressed EMT and arrested ingressive cell movement in the chick VER. Mice mutant in *noggin* displayed dysregulation of EMT with continued ingressive cell movement. These indicate that the inhibition of *Bmp* signaling by temporal and/or spatial *Nog* expression suppresses EMT and leads to the cessation of the ingressive cell movement from the VER at the end of gastrulation.

KEY WORDS: Chick, Mouse, *Bmp*, *Noggin*, Gastrulation, Epithelial-mesenchymal transition (EMT), Ventral ectodermal ridge (VER), Tail, Sonoporation

INTRODUCTION

During early embryogenesis, the primitive streak first appears as a thickening of the epiblast at the posterior marginal zone, the future caudal end of the embryo (Bellairs, 1986; Eyal-Giladi et al., 1991; Vakaet, 1984; Stern, 1990). The mediolateral intercalating cell movement and convergent extension is responsible for the progression of the primitive streak (Chuai et al., 2006; Lawson and Schoenwolf, 2001). The epiblast migrates toward the primitive streak and ingresses through the primitive groove to become the definitive endoderm and mesoderm. Such ingressing cells undergo epithelial-mesenchymal transition (EMT) and migrate into the blastocoel to form the mesodermal layer including the presomatic mesoderm (PSM), intermediate mesoderm and lateral plate mesoderm corresponding to the head-trunk region along the anterior-posterior (AP) axis (Shook and Keller, 2003). This developmental process is referred as gastrulation.

Several bone morphogenetic protein (*Bmp*) genes (e.g. *Bmp2*, *Bmp4*, *Bmp7*) are expressed adjacent to the primitive streak, and BMP signaling has been shown to be essential for mesoderm formation from the gastrula to the somitogenesis stage (Komatsu et al., 2007; Mishina et al., 1995; Ohta et al., 2004). In addition, BMP signaling can induce EMT during the formation of neural crest (Liem, Jr et al., 1995; Liu and Jessell, 1998). The regulatory

mechanism of EMT has been shown to involve the direct suppression of E-cadherin expression by Snail (*Slug*), one of the zinc-finger transcription factors (Batlle et al., 2000; Bolos et al., 2003; Cano et al., 2000). Consequently, epithelial cells acquire mobility through the reduction of cell-cell adhesion and differentiate into mesenchymal cells.

The primitive streak and Hensen's node are replaced by a bulb-like structure, the tailbud, consisting of a morphologically uniform mass of mesenchyme, during the late gastrula stage (Schoenwolf, 1979a; Schoenwolf, 1981). The late primitive streak contributes to the ventral ectodermal ridge (VER) which is the thickened ectodermal tissue located at the tailbud ventrodistally, following the caudal elongation of the tailbud (Catala et al., 1995; Schoenwolf, 1981; Tam and Beddington, 1987; Wilson and Beddington, 1996). The histological similarity between the VER and the apical ectodermal ridge (AER) suggests that the VER is the signaling center for tail development and it positively regulates tail elongation through modulating proliferation of mesodermal cells during tail development (Cohn and Tickle, 1996; Globus and Vethamany Globus, 1976; Gruneberg, 1956; Reiter and Solursh, 1982). However, there is no direct evidence that the VER directly regulates the proliferation of mesodermal cells (Goldman et al., 2000).

Gastrulation is a fundamental process of embryogenesis and many studies have investigated the developmental mechanism of the initiation, induction and/or patterning of mesoderm during gastrulation. However, the developmental processes at the end of gastrulation have not been elucidated so far. Since the VER is derived from the primitive streak of late gastrula stage, histological and genetic analyses of the VER are expected to reveal the developmental mechanisms at the end of gastrulation. This study identified one of the regulatory mechanisms controlling the cessation of ingressive cell movement from the VER at the end of gastrulation.

¹Center for Animal Resources and Development (CARD), Graduate School of Medical and Pharmaceutical Sciences, Kumamoto University, Honjo 2-2-1, Kumamoto 860-0811, Japan. ²JSPS research fellow, Chiyoda-ku 1-8, Tokyo 102-8472, Japan. ³Department of Anatomy, Fukuoka University School of Medicine, Fukuoka, Japan. ⁴Department of Developmental Neurobiology Graduate School of Medical Sciences, Kumamoto University, Honjo 2-2-1, Kumamoto 860-0811, Japan.

*Author for correspondence (e-mail: gensen@gpo.kumamoto-u.ac.jp)

MATERIALS AND METHODS

Animals

Fertilized White Leghorn chicken eggs were purchased from Marui Farm (Izumi, Japan). Eggs were incubated at 38.5°C and staged according to the Hamburger and Hamilton classification (Hamburger and Hamilton, 1951). *noggin* (*Nog*) mutant mice have been previously described (Brunet et al., 1998; McMahon et al., 1998; Bachiller et al., 2000; Suzuki et al., 2003).

In situ hybridization for gene expression analysis

Whole-mount in situ hybridization was performed by standard procedures using probes for mouse (*m*) *Bmp2*, chicken (*c*) *Bmp2*, *cBmp4*, *cBmp7*, *mBmp7* and *cNog* (Haraguchi et al., 2000) (kindly provided by B. L. Hogan, Duke University Medical Center, Durham, NC; T. Nohno, Kawasaki Medical School, Kurashiki, Japan; C. Tickle, University of Dundee, UK; B. Houston, University of Dundee, UK; M. Yoshida, IMEG, Kumamoto, Japan; and Y. Takahashi, Nara Institute of Science and Technology, Nara, Japan, respectively), *mBmp4* (Jones et al., 1991), *mNog* (McMahon et al., 1998). Section in situ hybridization was performed by standard procedures using probes of *mSnail* (*Snail*) and *cSlug* (kindly provided by A. Nieto, Instituto Cajal, Madrid, Spain, and H. Tanaka, Kumamoto University, Kumamoto, Japan).

Developmental cell fate analysis

DiI (1,1'-dioctadecyl-3,3,3',3'-tetramethylindocarbocyanine perchlorate; Molecular Probes) was used as a fluorescent lineage labeling reagent at a concentration of 0.05% in 0.3 M sucrose to label both mouse and chick ectoderm including the VER. The culture of mouse tail grafts was performed as described previously (Goldman et al., 2000).

Immunohistochemistry

Paraffin sections of embryos fixed in 4% paraformaldehyde (PFA) were prepared with a microtome (MICROM, Germany). Immunostaining was performed by standard procedures. The specimens were incubated at 4°C overnight with the following primary antibodies: anti-GFP antibody (mouse monoclonal, Roche); anti-E-cadherin (mouse monoclonal, BD Bioscience); anti-laminin (rabbit monoclonal, Sigma); anti-pSmad1.5.8 antibody (rabbit polyclonal, Cell Signaling Technology). After three washes with PBST, the specimens were subsequently incubated with the following secondary antibodies diluted 1:200 in a solution of PBST containing 0.2% fetal bovine serum (FBS): Alexa Fluor 488 goat anti-mouse IgG or Alexa Fluor 568 goat anti-rabbit IgG (Molecular Probes).

In ovo sonoporation

The full-length *mNog* cDNA subcloned in pCAB-IRES-GFP expression vector was used for in ovo sonoporation studies (pCAB-IRES-GFP was kindly provided by A. Tucker, King's College London, UK). Optison (Mallinckrodt, San Diego, CA, purchased from Nepagene, Japan) was used as a microbubble solution for gene transduction. For the preparation of DNA-microbubble, 10 µl of a plasmid DNA solution (concentration 2.0–4.0 µg/µl), such as pCAB-IRES-GFP, pCAB-*mNog*-IRES-GFP, pCAGGS-GFP, pCAGGS-*hBMP2* (the full-length human *BMP2* cDNA was kindly provided by S. Noji and H. Ohuchi) was added with 10 µl of Optison. The DNA-microbubble mixture was injected into the caudal end of the chick tailbud with a glass micro-needle (GD-1.2; Narishige, Tokyo, Japan). The injected chick embryos were immediately exposed to ultrasound using a 3 mm diameter ultrasound probe (Sonitron 2000N, Rich Mar, Inola, OK, purchased from Nepagene) with an input frequency of 1 MHz, an output intensity of 2.0 W/cm², a pulse duty ratio of 20% for a duration of 60 seconds (Ohta et al., 2003; Ohta et al., 2007).

RESULTS

Development of the tailbud and the VER

The formation of the tailbud and the VER during the processes of chick embryogenesis is illustrated in Fig. 1A. During the late gastrula stage when the posterior neuropore remains unclosed, tailbud formation is initiated at the caudal end of the embryo from HH stage 11–12 (Schoenwolf, 1979a). The tailbud is prominently observed as a mass of mesenchyme until HH stage 13–14 when the

posterior neuropore completely closes (Schoenwolf, 1979b). The remnant of the regressed primitive streak exists at the caudal end of chick embryo (the red region at HH stage 14 in Fig. 1A) (Knezevic et al., 1998; Schoenwolf, 1979a). Previous fate map analyses demonstrated that the remnant of the primitive streak contributes to the VER (Catala et al., 1995; Schoenwolf, 1981; Tam and Beddington, 1987; Wilson and Beddington, 1996). Accompanying the elongation of the tailbud, the remnant of the primitive streak is progressively involuted toward the ventral region of the tailbud, resulting in the formation of the chick VER in the ventral tail region during HH stage 16–18 (the blue region at HH stage 16 and 18 in Fig. 1A) (Catala et al., 1995; Mills and Bellairs, 1989). It is thought that the chick VER finally disappears through cell death by the stage when most of the somites have formed (HH stage 24, Fig. 1A) (Miller and Briglin, 1996).

Fate mapping and histological analysis of the chick VER

The histogenesis of the chick VER and its adjacent tissues was examined during HH stage 17–18 (Fig. 1B). The chick embryonic tail is composed of the neural tube, the notochord, the presomatic mesoderm, the tail gut, the tail ventral mesoderm (TVM) and the VER (Fig. 1C). Histological observations revealed that a portion of the ectodermal cells in the chick VER appeared to migrate toward the tailbud mesodermal region (Fig. 1D). Immunostaining for E-cadherin and laminin showed degradation of the basal membrane underlying the chick VER (arrowheads in Fig. 1E), thus suggesting that the chick VER undergoes EMT.

It has been reported that the regressed streak during the late gastrula stage (HH stage 11–13) displays gastrulation-like ingressive movement in chick embryos (Knezevic et al., 1998). Further fate map analyses were performed to examine whether the chick VER continuously displays gastrulation-like ingressive cell movement. The ectoderm, including the chick VER, was labeled with DiI in HH stage 16–21 chick embryos. After 20–24 hours of the incubation, the DiI-labeled cells in the HH stage 16–19 chick embryos were observed in the ventrolateral region of tailbud (HH stage 16, Fig. 1F; *n*=17/18; data not shown). The labeled cells were located in the ventrolateral mesoderm of the tailbud (arrows in Fig. 1F, HH stage 16; *n*=15/16), thus indicating that gastrulation-like ingressive cell movement occurred continuously after the regression of the streak, contributing to form the chick VER. By contrast, few labeled cells were detected in the mesoderm when chick embryos were labeled at HH stage 20–21 (Fig. 1F, HH stage 20; *n*=15/16). Hence, the current histological and fate map analyses indicated that the chick VER undergoes EMT during the early tailbud stage (HH stage 16–19) and displayed gastrulation-like ingressive cell movement. Such cell movement is gradually attenuated and finally ceased around HH stage 21–24.

The expression pattern of *Bmp*(s) and the formation of the basal membrane during the chick tail development

The expression pattern of *Bmp* genes and their antagonists were examined in the chick tailbud. *cBmp4* was expressed in the ventral region of the tail gut and the TVM underlying the chick VER (Fig. 2A,D). *cBmp7* was expressed predominantly in the ventral ectoderm (Fig. 2B,E). The expression of *Bmp* antagonists (e.g. chordin, gremlin and follistatin) was not detected in or adjacent to the VER of chick embryos (data not shown). By contrast, *cNog* expression was observed in the ventral region of the tailbud, the neural tube and the notochord (Fig. 2C). Histological observations revealed that

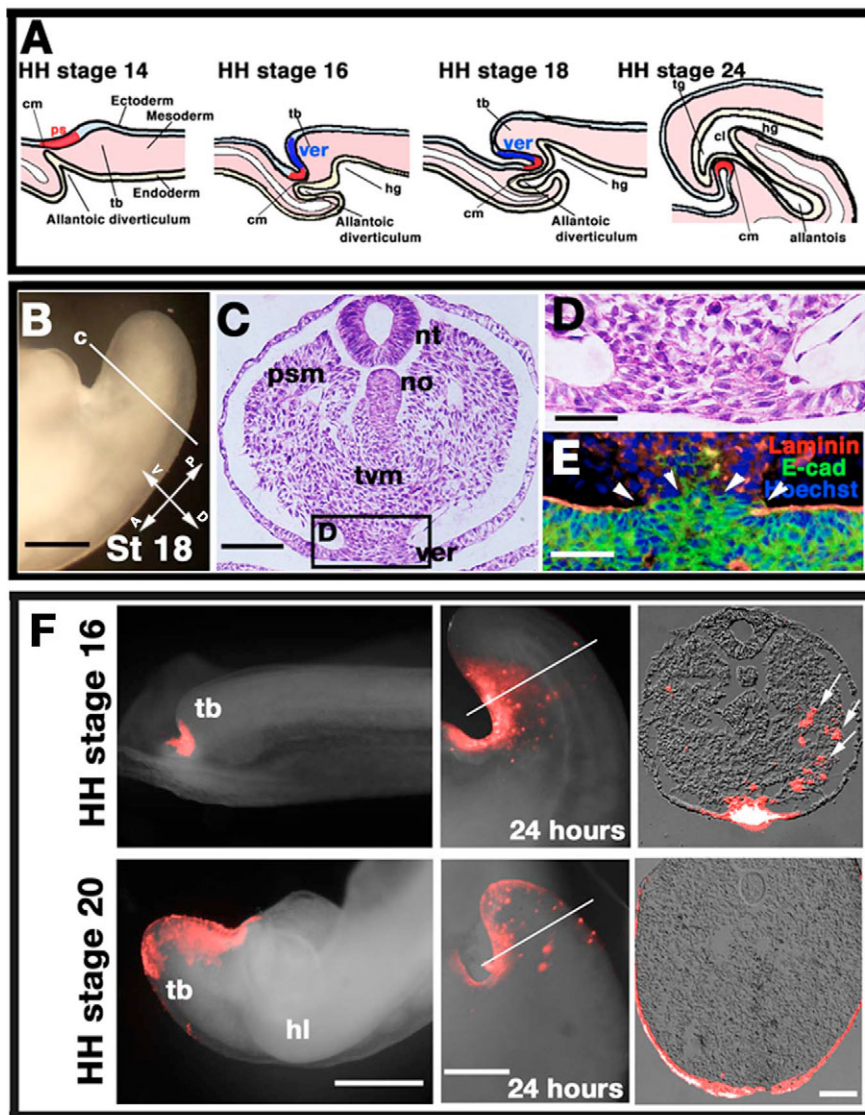


Fig. 1. Histological and fate map analysis of chick tail development. (A) A schematic illustration of chick caudal embryogenesis. cl, cloaca; cm, cloacal membrane; hg, hind gut; ps, primitive streak; tb, tailbud; ver, ventral ectodermal ridge. (B) The tailbud of chick embryos at HH stage 18. The white line in B indicates the approximate level of the section shown in C. Scale bar: 400 μm . (C) Transverse section of the chick tailbud. nt, neural tube; psm, presomatic mesoderm; tvmm, tail ventral mesoderm. Bar: 100 μm . (D) High magnification of the box in C, showing the chick VER and the adjacent region. Scale bar: 50 μm . (E) Immunostaining with laminin and E-cadherin of the chick VER. Bar: 50 μm . (F) Fate mapping of the tailbud ectoderm including the chick VER. The ectoderm was labeled with Dil at HH stage 16 and 20 (left panels). Middle and right panels show distribution of labeling after 24 hours. The white line in the middle panels indicates the position of the sections shown on the right. hl, hind limb. Scale bars: whole mounts, 800 μm , 400 μm ; sections, 100 μm .

cNog was prominently expressed in the ventrolateral region rather than in the midline of the TVM (arrow in Fig. 2F). The low level *cNog* expression in the midline of the TVM corresponded to the region where the basal membrane degradation was observed (Fig. 1E and Fig. 2F). To address the correlation between the *cNog* expression pattern and the basal membrane degradation, the kinetics of *cNog* expression and basal membrane degradation were examined during tail development in the chick. Before the posterior neuropore closure (around HH stage 10), *cNog* was expressed at Hensen's node, the notochord and neuroectoderm (data not shown) (Chapman et al., 2002). There was no *cNog* expression in the primitive streak and basal membrane degradation was evident at this stage (an arrow in Fig. 2G, HH stage 10; $n=10/10$). When the tailbud starts to elongate caudally after the posterior neuropore closure, *cNog* expression was initiated at the lateral-ventral region of the TVM (black arrowheads in Fig. 2G, HH stages 17 and 18; $n=28/29$). The degradation of the basal membrane was observed in the area overlapping the faint *cNog* expression in the midline of the TVM (white arrowheads in Fig. 2G, HH stage 17 and 18; $n=16/16$). *cNog* expression gradually expanded to the entire TVM until HH stage 24–25 (HH stage 24, Fig. 2G; $n=12/12$). The basal membrane degradation was not observed at HH stage 24–25 coinciding with

such *cNog* expression in the entire TVM (HH stage 24, Fig. 2G; $n=11/13$). Taken together, we hypothesized that EMT in the chick VER is induced by BMP signaling and it is thus suppressed through the inhibition of BMP signaling by temporal and/or spatial *cNog* expression at the end of gastrulation.

Gene transduction into the chick tailbud using sonoporation (in ovo sonoporation)

To examine the hypothesis suggested above, *Nog* expression vector was transduced into the ventral tail region. Sonoporation was used for gene transduction because of its efficacy for transduction without significant embryonic damage (Ohta et al., 2003; Tachibana and Tachibana, 1995). GFP expression was already observed 3 hours after sonoporation in the caudal region of the chick embryos (Fig. 3B; $n=155/160$), where positive cells were detected among the ingressing cells and the ectoderm of the streak (Fig. 3C; $n=12/14$). Twelve hours after sonoporation, GFP expression was prominent at the ventral region of the developing tailbud (Fig. 3D; $n=40/42$), where positive cells were detected adjacent to the chick VER (Fig. 3E; $n=13/14$). Approximately 60–70% of the treated embryos survived without significant morphological abnormalities of the tail for 7 days after gene transduction (data not shown).

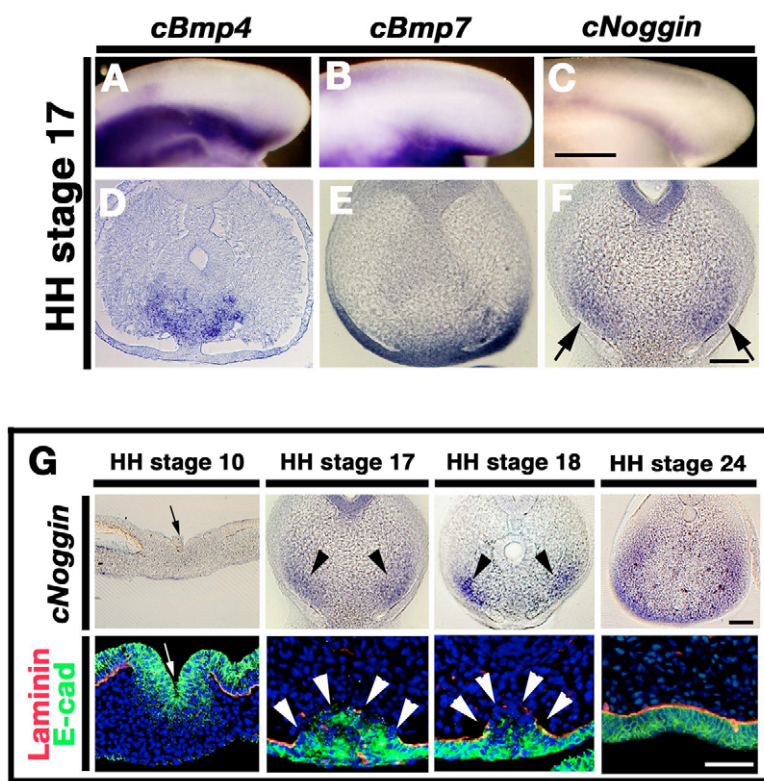


Fig. 2. *Bmp(s)* and *Nog* expression pattern and degradation of the basal membrane. Gene expression analysis for the tailbud at HH stage 17. (A,D) *cBmp4*, (B,E) *cBmp7*, (C,F) *cNog*. Arrows indicate expression in the ventrolateral region. Scale bars: 400 μm (A-C); 100 μm (D-F). (G) The kinetics of the *cNog* expression pattern and basal membrane degradation. The arrow indicates the primitive groove. Note that *cNog* is expressed in the ventrolateral region of the TVM at HH stage 17-18 (black arrowheads) and that basal membrane degradation occurs where there is a low level of *cNog* expression (white arrowheads). Until HH stage 24, *cNog* expression extended to the entire TVM and the basal membrane was formed along the entire ventral ectoderm. Scale bars: 100 μm .

***Nog* overexpression inhibits EMT in the chick VER**

Nog-overexpressing chick embryonic tails were narrower dorsoventrally than those of the control embryos (Fig. 3F; $n=24/30$). To examine the alteration of gastrulation-like ingressive cell movement from the chick VER, the surface ectoderm including the chick VER was labeled with DiI and the *mNog* expression vector was transduced into the caudal region of chick tailbud at HH stage 15-16 (Fig. 3G). DiI-labeled cells in *Nog*-overexpressing embryos localized only in the ventral ectoderm, resulting in a dramatic decrease of the tailbud mesoderm after 24 hours (HH stage 20, Fig. 3G; $n=15/18$). These results indicated that *Nog* overexpression induced the arrest of gastrulation-like ingressive movement from the chick VER.

Nog overexpression was further examined to determine whether it inhibited EMT in the chick VER. The control embryos showed no significant abnormalities, whereas epithelial cells accumulated in the midline of ventral ectoderm of *Nog*-overexpressing embryos (Fig. 3H,I; $n=23/25$). GFP-positive cells were detected in the ventral tail region of both control and *Nog*-overexpressing chick embryos (Fig. 3J,K; $n=12/12$). pSmad signals were localized in the nucleus of the ectodermal cells including the control VER or the juxtaposed mesoderm (Fig. 3L,L'). However, the number of pSmad positive cells was remarkably decreased in the ventral ectoderm of *Nog*-overexpressing embryos (Fig. 3M,M'; $n=8/13$). Control embryos showed basal membrane degradation underlying the chick VER, and *cSlug* was expressed adjacent to the site of the basal membrane degradation (Fig. 3N,P; $n=10/10$). In contrast, *Nog*-overexpressing chick embryos formed a basal membrane surrounding abnormally accumulating ectodermal cells in the midline of the ventral ectoderm with considerably decreased *cSlug* expression (Fig. 3O,Q; $n=13/15$). These results demonstrate that EMT in the chick VER was inhibited by *Nog* overexpression, suggesting that decreased BMP signaling adjacent to the chick VER leads to the arrest of gastrulation-like ingressive cell movement though suppressing EMT.

Bmp2* overexpression induces breakdown of the basal membrane and upregulation of *cSlug

In order to confirm the results of *Nog* overexpression, the ability of *Bmp* overexpression to induce EMT at the stage coinciding with the cessation of gastrulation was examined. Intriguingly, when *Nog* was overexpressed, endogenous *cBmp2* expression was upregulated in the accumulating epithelial cells (data not shown). It has been suggested that a factor secreted from the VER, such as *Bmp2*, maintains the mesenchymal expression of *Nog* (Goldman et al., 2000). This implies that a feedback loop may exist between *cNog* and *cBmp2*, and that *cBmp2* could be a candidate to induce EMT in the chick VER. Normally, the ingressive cell movement ceases until HH stage 23-24, as judged by laminin staining (Fig. 4A,C; $n=16/18$). However, human *BMP2*-overexpressing embryos displayed the breakdown of basal membrane accompanied by the decrease of E-cadherin expression at HH stage 23-24 (Fig. 4B,D; $n=10/12$). Furthermore, upregulation of *cSlug* was also observed in *hBMP2*-overexpressing embryos (Fig. 4E,F; arrows; $n=5/18$).

The arrest of ingressive cell movement leads to the caudal body malformation in chick embryos

Chick-quail transplantation experiments revealed that the descendant cells from the late primitive streak and its derivative, the chick VER, contribute to the caudal body including the tail and external genitalia (data not shown) (Catala et al., 1995). This suggested that the mesoderm supply from the late primitive streak and the VER is essential during the chick caudal body formation. When *Nog* was overexpressed in the caudal end of the tailbud after the posterior neuropore closure (HH stage 15-16), the ingressive cell movement was arrested until HH stage 18-19 (data not shown; $n=4/5$). In fact, *Nog*-overexpressing chick embryos displayed tail truncation with defects of the caudal vertebrae including the coccyx after 7-8 days of incubation (Fig. 5A-D; $n=24/30$). The external

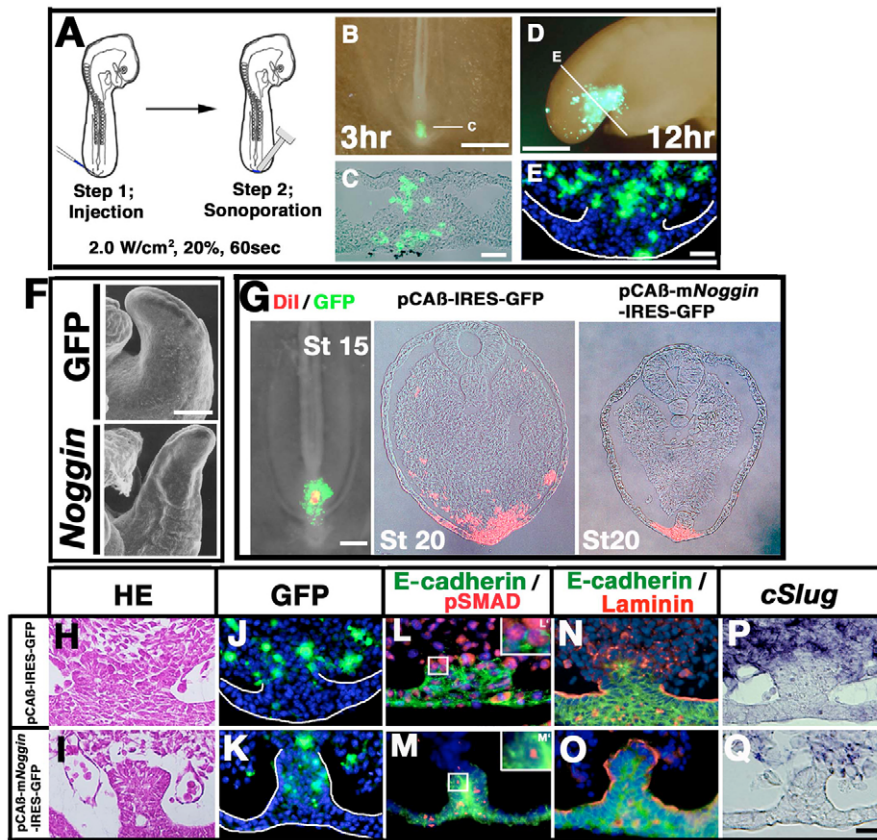


Fig. 3. *Nog* overexpression in the tailbud using sonoporation. (A) A schematic drawing of the sonoporation procedure. (B-E) GFP expression after Sonoporation. The white lines in B and D indicate the position of the sections in C and E. Scale bars: 400 μm (B,D); 50 μm (C,E). (F) Morphology of the tailbud of control and *Nog*-overexpressing chick embryos. Scale bar: 200 μm . (G) pCAB-IRES-GFP or pCAB-mNoggin-IRES-GFP were transduced into the caudal region of the chick tailbud. The surface ectoderm of the tailbud was labeled with Dii after sonoporation. The distribution of Dii-labeled cells in control and *Nog*-overexpressing embryos was observed after 24 hours. Scale bars: 200 μm (left); 100 μm (middle and right). (H,I) Hematoxylin and Eosin staining of control and *Nog*-overexpressing embryos. (J,K) GFP expression in control and *Nog*-overexpressing embryos. (L,M) Immunostaining of pSmad (red) and E-cadherin (green) in control and *Nog*-overexpressing embryos. (L',M') High-magnification view of boxed area in L and M. (N,O) Immunostaining of E-cadherin (green) and laminin (red) in control and *Nog*-overexpressing embryos. (P,Q) *cSlug* expression in control and *Nog*-overexpressing embryos. Scale bar: 50 μm .

genitalia of chick embryos are normally composed of the genital (cloacal) tubercle surrounded by the sulcus phalli (HH stages 32-35, Fig. 5E) (Bakst, 1986). *Nog*-overexpressing chick embryos showed hypoplasia of the sulcus phalli (Fig. 5F; $n=20/28$), although the genital tubercle formation appeared unaffected. It has been suggested that there is a close association between the development of the hind gut and the tail (de Santa Barbara and Roberts, 2002; Gruneberg, 1956). This is consistent with the current observation of a malformation of the hind gut including the cloaca and the tail gut in *Nog*-overexpressing chick embryos (Fig. 5G,H; $n=8/14$). In addition, a severe phenotype with both hind limbs fused proximally was occasionally observed (Fig. 5I,J; $n=2/30$).

Histological analysis of the mouse VER

The process of VER formation in mouse embryos appears to be similar to that in chick embryos (Tam and Tan, 1992; Wilson and Beddington, 1996). The mouse VER is thought to be derived from the primitive streak of the late gastrula stage (Tam and Beddington, 1987). Its formation is initiated at the early tailbud stage when the closure of the posterior neuropore begins (around E9.0, data not shown) (Gofflot et al., 1997; Goldman et al., 2000; Wilson and Beddington, 1996). During this stage, the ventral ectoderm derived from the late primitive streak displays no significant thickening on the ventral side of the tailbud (data not shown). A previous fate map analysis revealed that ingressive cell movement occurs continuously until the closure of the posterior neuropore is complete (Wilson and Beddington, 1996). After the posterior neuropore closure, the mouse VER is evident as a thickened surface ectoderm on the ventral side of the tailbud (Fig. 6A-C). It has been suggested that the ectoderm of the mouse VER contains progenitor cells contributing to the midline of the ventral ectoderm of the tail (Goldman et al., 2000). In

fact, when mouse ventral ectoderm, including the VER, was labeled with Dii and the labeled tail grafts were subsequently cultured, the labeled cells in the tail grafts localized along the AP axis of the

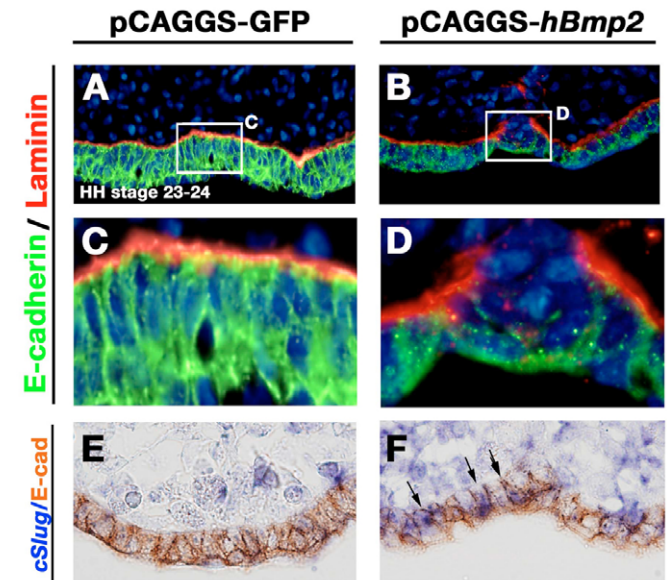


Fig. 4. *Bmp2*-overexpression in chick embryos. (A,B) Immunostaining of E-cadherin (green) and laminin (red) in GFP and human *BMP2* (*hBmp2*)-overexpressing embryos. (C,D) High-magnification view of boxed area in A and B. (E,F) Double-staining for *cSlug* (blue) and E-cadherin (brown) of GFP or *hBmp2*-overexpressing embryos. Note that the cells expressing both *cSlug* and E-cadherin are in the ventral ectodermal layer in the *BMP2*-overexpressing embryos (arrows).

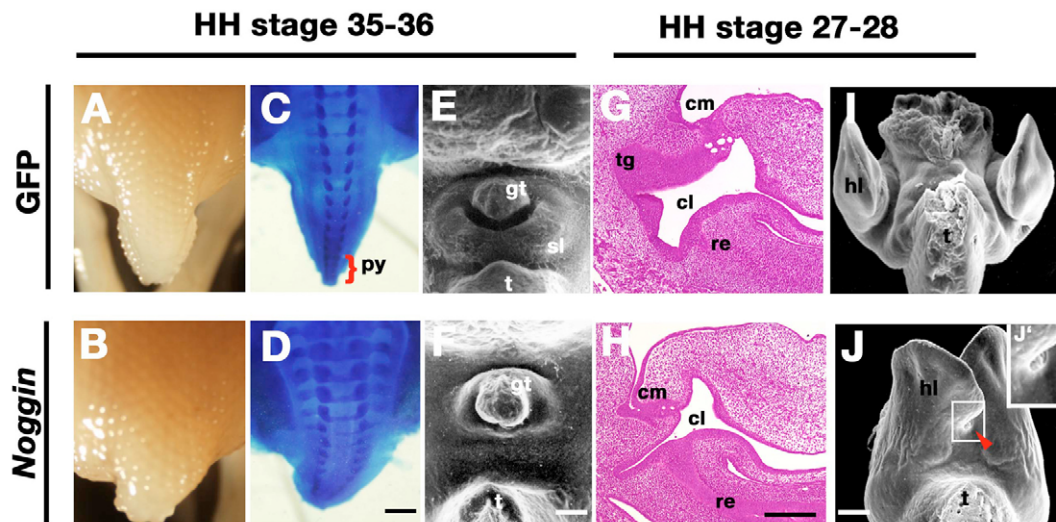


Fig. 5. The caudal dysmorphogenesis induced by *Nog* overexpression. (A,B) Dorsal view of the tail of control and *Nog*-overexpressing chick embryos at HH stage 35-36. (C,D) Skeletal pattern of the tail in control and *Nog*-overexpressing chick embryos. py, pygostyle. Scale bar: 800 μ m. (E,F) Frontal view of the external genitalia of control and *Nog*-overexpressing chick embryos. gt, genital tubercle; sl, sulcus phalli; t, tail. Scale bar: 200 μ m. (G,H) Histological analysis of the hind gut region of control and *Nog*-overexpressing chick embryos. Cl, cloaca; cm, cloaca membrane; re; rectum; tg, tail gut. Scale bar: 100 μ m. (I,J) Hind limb fusion (arrowhead) in *Nog*-overexpressing chick embryos. hl; hind limb; t; tail. Scale bar: 200 μ m. (J') High magnification of the boxed area in J.

ventral midline surface of the tailbud after 20-24 hours (data not shown) (Goldman et al., 2000). In addition, an analysis of E-cadherin and laminin expression revealed no significant basal membrane degradation in the mouse VER (Fig. 6D; $n=14/16$). These data imply that the ingression from the ventral ectoderm continues at least until around E9.0-9.5 and ceases thereafter.

The pattern of *Nog* expression and basal membrane degradation during the mouse tail formation

mBmp4 expression was detected in the tail gut and the TVM (data not shown) (Goldman et al., 2000). *mBmp2* was specifically expressed along the entire length of the mouse VER (data not

shown) (Goldman et al., 2000). *mNog* expression was observed in the entire TVM underlying the mouse VER (Fig. 6E) (Goldman et al., 2000). To address whether the regulatory mechanisms of the EMT at end of the gastrulation are conserved in mouse tail development, the kinetics of *mNog* expression and basal membrane degradation were examined during this process. Before the posterior neuropore closure (E8.5), *mNog* expression is detected in the notochord and the dorsal neural tube (Bachiller et al., 2000; Brunet et al., 1998; Li et al., 2007; McMahon et al., 1998). Basal membrane degradation was observed at the primitive streak (an arrow at E8.5, Fig. 6E; $n=10/10$). In the early tailbud stage at E9.0 (before the posterior neuropore closure), a low level of *mNog* expression was observed in the TVM (red arrowhead at

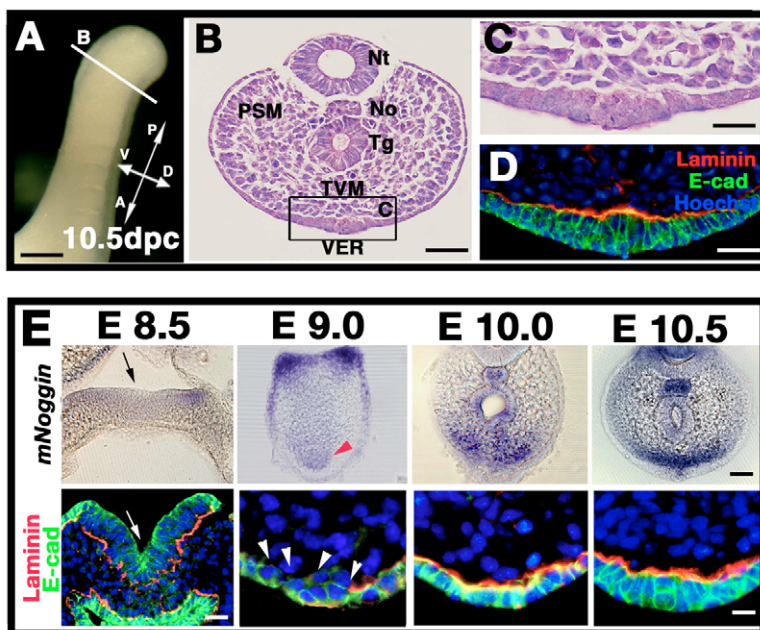


Fig. 6. A histological analysis of the mouse VER and kinetics of *mNog* expression pattern and basal membrane degradation during mouse tail development. (A) The tailbud of a mouse embryo at E10.5. The white line indicates the approximate level of the section shown in B. Scale bar: 400 μ m. (B) Transverse section of the mouse tailbud. No, notochord; Nt, neural tube; PSM, presomatic mesoderm; Tg, tail gut; TVM, tail ventral mesoderm; VER, ventral ectodermal ridge. Scale bar: 100 μ m. (C) High magnification of the boxed region in B. Scale bar: 50 μ m. (D) Immunostaining with laminin (red) and E-cadherin (green) of the mouse VER. Scale bar: 50 μ m. (E) The kinetics of *mNog* expression pattern and basal membrane degradation. An arrow indicates the primitive groove. Scale bar: 50 μ m. Note the low level *mNog* expression in the TVM at E9.0 (red arrowhead) and the associated basal membrane degradation underlying the ectoderm derived from the late primitive streak (white arrowheads). Prominent *mNog* expression was localized in the TVM and basal membrane was formed underlying the mouse VER until E10.0-10.5. Scale bars: black, 50 μ m; white, 10 μ m.

E9.0, Fig. 6E; $n=15/15$). Immunostaining of laminin and E-cadherin revealed the degradation of basal membrane underlying the ventral ectoderm during the early tailbud stage (white arrowheads at E9.0, Fig. 6E; $n=10/11$). *mNog* expression became gradually stronger during the tailbud outgrowth and continued in the entire TVM until the disappearance of the VER at E13.0 (E10.0-10.5, Fig. 6E; $n=22/24$; data not shown). The degradation of the basal membrane underlying the mouse VER was not observed after the posterior neuropore closure (E10.0-10.5, Fig. 6E; $n=18/18$). These data suggested that EMT in the ventral ectoderm occurs continuously until E9.0-9.5 and that temporal and/or spatial *mNog* expression may be involved in the suppression of EMT.

***Nog* mutant mice display aberrant EMT during the tail formation**

To examine the developmental functions of *mNog* in the regulation of the EMT of mouse VER, we addressed whether the ventral ectoderm of the tailbud undergoes EMT in *Nog* mutant mice. There were no significant morphological differences between wild-type and *Nog* mutant mice in the caudal region containing the tailbud before the posterior neuropore closure (data not shown) (McMahon et al., 1998). However, after the posterior neuropore closure (E10.0), *Nog* mutant mice displayed a slightly short and thickened tailbud compared with that of the wild-type mouse (Fig. 7A,B). A histological analysis revealed an increase of tailbud mesoderm in *Nog* mutant mice (Fig. 7C,D; $n=11/12$). There were no significant differences in cell proliferation in the tailbud mesoderm based on BrdU incorporation analysis between the two mice (data not shown). In addition, *Nog* mutant mice lacked apparent ectodermal cells corresponding to the prospective mouse VER region (Fig. 7E,F; $n=6/8$). A few apoptotic signals were mainly detected at the TVM in the stage of early VER formation in *Nog* mutant mice (data not shown), suggesting that aberrant EMT, responding to the elevated Bmp signaling, leads to the absence of apparent ectodermal cells, excluding the possibility of apoptotic influences. In fact, both pSmad-positive cells and loss of laminin and E-cadherin expression were observed in such regions of *Nog* mutant mice (arrowheads in Fig. 7G,H; $n=4/5$, arrowheads in Fig. 7I,J; $n=3/4$). Furthermore, an increase of *mSnail* expression was observed at the ventral region corresponding to the decrease of E-cadherin expression in *Nog* mutant mice (arrowheads in Fig. 7K,L; $n=3/4$). Dil labeling experiments revealed the presence of cell migration from the ventral ectoderm to the tailbud mesoderm in *Nog* mutant mice (Fig. 7M,N; $n=4/5$). These results suggested that *Nog* mutant mice exhibited an ingressive cell movement in response to the increased Bmp signaling even after posterior neuropore closure, and that *mNog* expression is required to suppress EMT in the mouse VER.

DISCUSSION

Gastrulation is a fundamental and complex process during early embryonic development. It involves cellular commitment and movement whereby the three fundamental germ layers (ectoderm, mesoderm and endoderm) are established in vertebrate embryos. To understand the molecular mechanisms underlying gastrulation, a number of studies have focused on the molecules initiating gastrulation and/or the cellular behaviors during gastrulation. However, the developmental mechanism that regulates the end of gastrulation has not yet been elucidated. This is the first study to characterize one of the regulatory mechanisms for the cessation of gastrulation in amniotes.

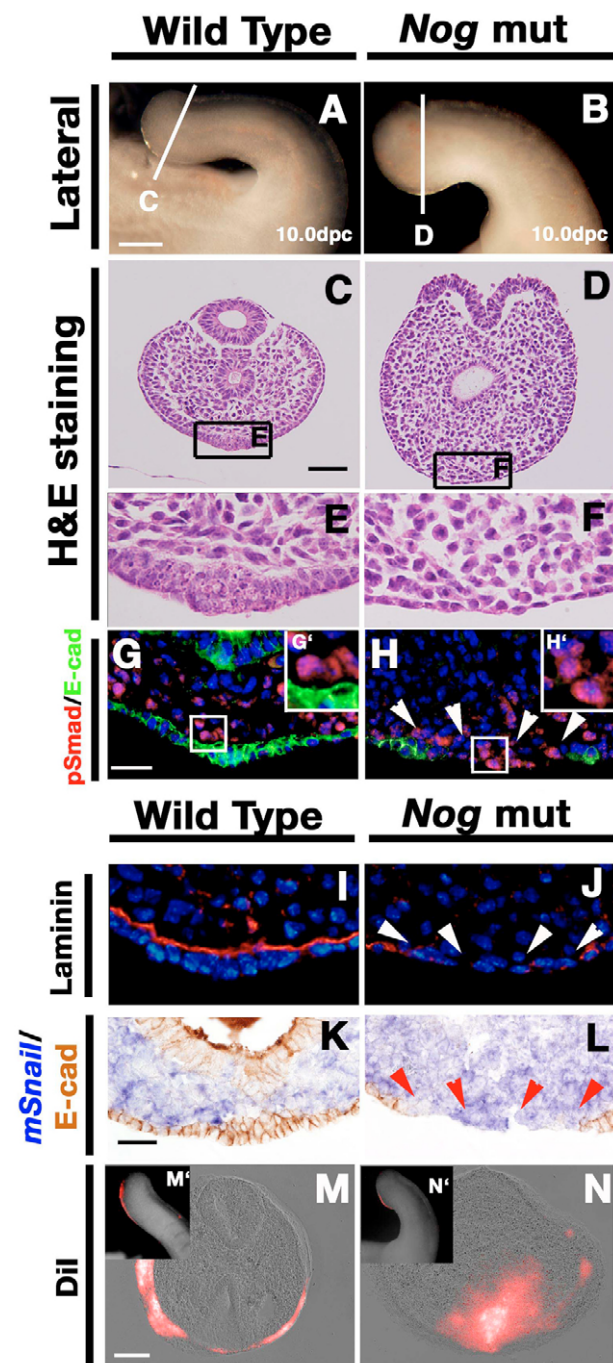


Fig. 7. Phenotypic analyses of *Nog* mutant mice. (A,B) Lateral view of the tailbud in wild-type and *Nog* mutant mice at E10.0. Scale bar: 800 μm . (C,D) Hematoxylin and Eosin staining of tailbud sections of wild-type and *Nog* mutant mice. Scale bar: 100 μm . (E,F) High magnification of the boxed region in C,D. (G,H) Immunostaining of pSmad (red) and E-cadherin (green). Note that pSmad signals were detected in the prospective VER region of *Nog* mutant mice, and that E-cadherin expression was negative in the same region (arrowheads). Scale bar: 50 μm . (G',H') High-magnification view of boxed area in G and H. Note that the pSmad signal is localized in the nuclei. (I,J) Immunostaining of laminin. (K,L) Double staining of *mSnail* (blue) and E-cadherin (brown). Note that *mSnail* was detected in the region without E-cadherin expression in *Nog* mutant mice (arrowheads). Scale bar: 50 μm . (M,N) Distribution of Dil-labeled cells after 24 hours in culture. (M',N') Dil-labeling at the ventral surface ectoderm of the tailbud. Scale bar: 100 μm .

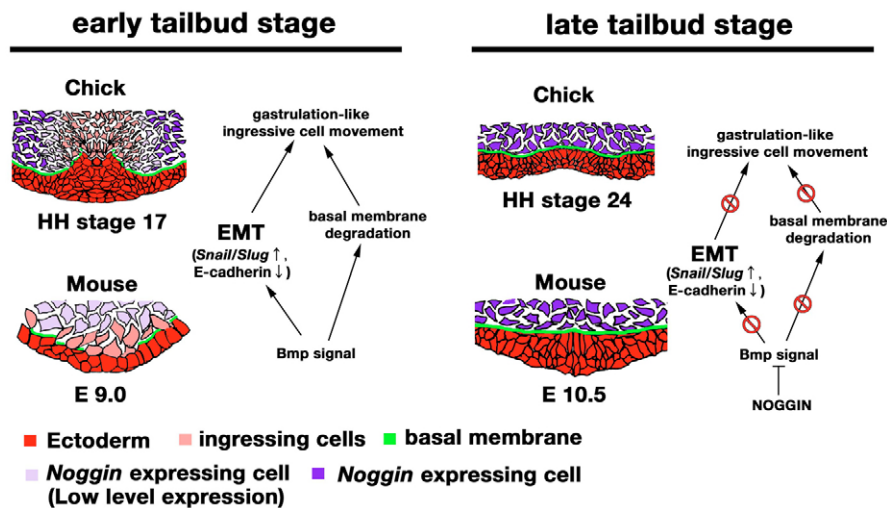


Fig. 8. Schematic diagram showing the cessation of gastrulation. During the early tailbud stage of chick embryos, *cNog* expression is initiated at the ventrolateral region of the TVM (purple indicated the *Nog*-expressing cells). BMP signaling could induce EMT with basal membrane (green) degradation. The chick VER shows gastrulation-like ingressive cell movement (pink indicates the ingressing cells). In the late tailbud stage of the chick embryos, *cNog* expression extends to the entire TVM (purple; the *Nog*-expressing cells) and inhibits Bmp signaling, which results in the suppression of EMT and basal membrane formation. In the early tailbud stage of mouse embryos, *mNog* expression in the TVM is low (light purple). The ectoderm derived from the late primitive streak shows ingressive cell movement with basal membrane degradation (pink indicates the ingressing cells and green indicates the basal membrane). In the late tailbud stage of mouse embryos, *mNog* is prominently expressed in the entire TVM (purple indicates the *Nog*-expressing cells) and inhibits BMP signaling, which results in the suppression of EMT and basal membrane formation.

Suppression of EMT occurs at end of gastrulation in amniotes

EMT is one of the crucial events during gastrulation. The expression of an induction factor for EMT and the degradation of the basal membrane in the primitive streak are fundamental processes necessary for gastrulation. In this context, the suppression of such induction factors and the negative regulation of degradation of basal membrane could be involved in the cessation of gastrulation.

TGF β signaling is required to promote EMT by induction of *Snail* family genes (Barrallo Gimeno and Nieto, 2005; Peinado et al., 2003). Bmps, members of TGF β super family, can also induce *Slug* expression during the neural crest formation in chick embryos (Liu and Jessell, 1998). Recently, the binding site of Smad1 has been identified in the promoter region of *Snail/Slug* (Sakai et al., 2005). Although the role of Smad in regulating *Snail/Slug* expression during gastrulation is still unclear, there is evidence that BMP signaling is involved in the regulation of EMT during gastrulation. Bmp genes, such as *Bmp2*, *Bmp4*, *Bmp7*, are expressed at the primitive streak along its AP axis (Chapman et al., 2002). pSmad expression is also detected in the ingressing cells at the primitive streak (Faure et al., 2002). *Bmpr1a*-null mutant mice cannot initiate gastrulation during early development (Mishina et al., 1995). *Bmp4* mutant mice display gastrulation defects and a failure to form sufficient mesoderm (Winnier et al., 1995). Similarly, *Bmp2* mutant mice show abnormalities in the formation of both extra-embryonic and embryonic mesodermal derivatives (Zhang and Bradley, 1996). In *Smad1*^{+/-}:*Smad5*^{+/-} double heterozygous embryos, the mesoderm is reduced (Arnold et al., 2006). These findings suggest that EMT could be mediated by Bmp signaling during gastrulation. The ectoderm derived from the late primitive streak continuously shows gastrulation-like ingressive cell movement and supplies mesodermal cells to the tailbud during the early tailbud stage in chick and mouse embryos. Several *Bmp* genes are expressed in the ventral region of the tailbud, indicating that the derivatives of the late primitive streak could

undergo EMT in response to Bmp signaling in both types of embryos during the early tailbud stage. Consistent with this, the ingressive cell movement was arrested by the inhibition of Bmp signaling utilizing *Nog* overexpression in early tailbud stage of chick embryos. This data suggest that a low level of *Nog* expression during the early tailbud stage appears to be insufficient to suppress EMT during this stage (Fig. 8). In addition, the failure to suppress ingressive cell movement in human *BMP2*-overexpressing chick embryos or in *Nog* mutant mice, suggests that the negative regulation of Bmp signaling by *Nog* is required for the cessation of gastrulation-like ingressive cell movement at the late tailbud stage (Fig. 8).

Degradation of the basal membrane is observed at the sites of EMT in various processes including organ and tissue regeneration and cancer metastasis (Barrallo Gimeno and Nieto, 2005; Lepilina et al., 2006; Thiery, 2002). During gastrulation, epiblast cells at the site of the primitive streak undergo EMT that is associated with basal membrane degradation (Bellairs, 1986; Harrison et al., 1991). These previous reports suggest that basal membrane degradation is necessary for ingressive cell movement. In fact, degradation of the basal membrane underlying the VER continued until the cessation of ingressive cell movement during tail formation in both mouse and chick embryos at the early tailbud stage (Fig. 8). The present study demonstrated that a clear correlation exists between the pattern of *Nog* expression and basal membrane degradation adjacent to the TVM in chick and mouse embryos. Furthermore, alteration of Bmp signaling is associated with the basal membrane degradation underlying the VER in the two species. These results suggest that reduction of Bmp signaling by temporal and/or spatial *Nog* expression in the TVM could suppress the basal membrane degradation (at the late tailbud stage in Fig. 8).

Bmp signaling functions through the crosstalk between various signaling pathways (e.g. Shh signaling, Wnt signaling) during organogenesis (McMahon et al., 2003; Nakashima et al., 2005). More detailed analyses, e.g. analysis of the downstream genes, are

required to elucidate the role of Bmp signaling during the cessation of gastrulation. Following the Bmp signaling, the regulation of the cessation of gastrulation is a complex event requiring the involvement of multiple factors such as *Snail/Slug* expression and the rearrangement of cytoskeletal proteins, such as actin. In addition, it appears that basal membrane formation is essential to control epithelial cell formation. Experiments utilizing embryoid bodies derived from ES cells suggest that the basal membrane induces the epiblast formation through the suppression of EMT (Fujiwara et al., 2007). These findings also indicate that basal membrane formation is required to suppress EMT at the end of gastrulation. As for basal membrane regulation, Matrix metalloproteases (MMPs) probably play a role in basal membrane degradation, since MMP2 has been demonstrated to be crucial for the regulation of the EMT in avian cardiogenesis (Song et al., 2000). It has been reported that Bmp7 induces *Mmp2* expression (Wang et al., 2006), suggesting that Bmp signaling may regulate the expression of *Mmp(s)*. Reduction of Bmp signaling may lead to the formation of basal membrane with the decrease of *Mmp* expression adjacent to the VER. These possibilities require further examination.

The current results provided a framework to understand the mechanisms involved in the cessation of gastrulation. These findings suggest that the inhibition of Bmp signaling by temporal and/or spatial *Nog* expression adjacent to the VER could suppress EMT concomitant with the basal membrane formation, thus resulting in the cessation of gastrulation-like ingressive cell movement from the VER at the end of gastrulation.

Dysregulation of cell ingression associated with the caudal regression syndrome

Caudal regression syndrome (OMIM 600145) is a complex human malformation syndrome affecting the caudal vertebra, the hind gut, external genitalia and the hind limb (Duhamel, 1961). In human embryology, it has been suggested that defects of the primitive streak during the late gastrula stage could be associated with caudal regression syndrome (Davies et al., 1970). In amniote embryos, the ingression of epiblast cells is controlled by sequential activation of *Hox* clusters (Imura and Pourquie, 2006), indicating that the precursor cells migrating from the late primitive streak contribute to the caudal body formation in human. Therefore, defects in the primitive streak during the late gastrula stage might induce a decrease of tailbud mesoderm. The exacerbating effects of excess all-trans retinoic acid (RA) administration for this syndrome have been documented in animal models (Chan et al., 2002). *Wnt3a* expression in the tailbud is downregulated by the administration of RA (Chan et al., 2002), suggesting that *Wnt3a* is involved in the pathogenesis of caudal regression syndrome. Indeed, *Wnt3a^{fl}/Wnt3a^{fl}* mice, which are hypomorphic mutants of *Wnt3a*, display caudal truncation with failure of posterior somite development (Greco et al., 1996). *Wnt3a* expression is localized at the primitive streak along the AP axis during gastrulation in mouse embryos (Takada et al., 1994). *Wnt3a* has been suggested to function in establishing the mesodermal precursors for the tailbud during gastrulation (Takada et al., 1994). Although caudal regression syndrome may be a variety of causes, previous analyses on RA-treated mice and/or *Wnt3a* mutant mice suggest the possibility that a decrease of the TVM, due to a failure of gastrulation, could be one of the causative elements.

In fact, several studies have also suggested that the TVM is necessary for caudal body development including tail, hind gut, external genitalia and hind limb formation (de Santa Barbara and Roberts, 2002; Tucker and Slack, 2004; Zakin et al., 2005; Pyati et al., 2006). Analyses of *Bmp7-Tsg* compound mutant mice indicate

that a decrease of Bmp signaling leads to hypoplasia of the TVM in amniotes (Zakin et al., 2005). Based on these reports, Bmp signaling may play a pivotal role in establishing the mesodermal cells localized in the TVM. The current study also demonstrated that overexpression of *Nog* induced a decrease of the tailbud mesoderm with the arrest of ingressive cell movement, resulting in defects of the caudal vertebrae, hind gut anomalies, hypoplasia of the external genitalia and hind limb fusion resembling those of caudal regression syndrome. These results suggest that decreased cell migration from the late primitive streak and its derivatives may be associated with caudal regression syndrome. To properly establish TVM, these mesodermal cells would be supplied though EMT induced by Bmp signaling during early tailbud stage. Thereafter, suppression of EMT is required to prevent the supply of excess mesodermal cells.

Intriguingly, some histological sections of human embryonic tails show that ectodermal cells of the human VER seem to ingress toward the tailbud mesodermal region (e.g. at Carnegie stage 12-13) (Muller and O'Rahilly, 2004). This suggests that the human VER may function as a source of mesodermal cells during tail formation and that the arrest of ingressive cell movement from the human VER might induce caudal regression syndrome. In order to elucidate the mechanism of caudal regression syndrome, the contribution of cells derived from the human VER should therefore be analyzed in future.

We especially thank Drs Richard Harland for his invaluable support. We also thank Drs Gary Schoenwolf, Andrew McMahon, Daniel Bachiller, Liz Robertson, Patrick Tam, Kiyotoshi Sekiguchi, Shinji Takada, Kunimasa Ohta, Eddy Robertis, Chin Chang, Abigail Tucker, John Fallon and Olivier Pourquie. This study was supported by a JSPS Research Fellowship for Young Scientists; by a Grant-in-Aid for Scientific Research on Priority Areas, by Mechanisms of Sex Differentiation; by General promotion of Cancer Research in Japan; by the Global COE 'Cell Fate Regulation Research and Education Unit', Kumamoto University; and by a Grant for Child Health and Development (17-2) from the Ministry of Health, Labour and Welfare.

References

- Arnold, S. J., Maretto, S., Islam, A., Bikoff, E. K. and Robertson, E. J. (2006). Dose-dependent Smad1, Smad5 and Smad8 signaling in the early mouse embryo. *Dev. Biol.* **296**, 104-118.
- Bachiller, D., Klingensmith, J., Kemp, C., Belo, J. A., Anderson, R. M., May, S. R., McMahon, J. A., McMahon, A. P., Harland, R. M., Rossant, J. et al. (2000). The organizer factors Chordin and Noggin are required for mouse forebrain development. *Nature* **403**, 658-661.
- Bakst, M. R. (1986). Embryonic development of the chicken external cloaca and phallus. *Scan. Electron Microsc.* **2**, 653-659.
- Barrallo Gimeno, A. and Nieto, M. A. (2005). The Snail genes as inducers of cell movement and survival: implications in development and cancer. *Development* **132**, 3151-3161.
- Battle, E., Sancho, E., Franci, C., Dominguez, D., Monfar, M., Baulida, J. and Garcia De Herberos, A. (2000). The transcription factor snail is a repressor of E-cadherin gene expression in epithelial tumour cells. *Nat. Cell Biol.* **2**, 84-89.
- Bellaïrs, R. (1986). The primitive streak. *Anat. Embryol.* **174**, 1-14.
- Bolos, V., Peinado, H., Perez Moreno, M. A., Fraga, M. F., Esteller, M. and Cano, A. (2003). The transcription factor Slug represses E-cadherin expression and induces epithelial to mesenchymal transitions: a comparison with Snail and E47 repressors. *J. Cell Sci.* **116**, 499-511.
- Brunet, L. J., McMahon, J. A., McMahon, A. P. and Harland, R. M. (1998). Noggin, cartilage morphogenesis, and joint formation in the mammalian skeleton. *Science* **280**, 1455-1457.
- Cano, A., Perez Moreno, M. A., Rodrigo, I., Locascio, A., Blanco, M. J., del Barrio, M. G., Portillo, F. and Nieto, M. A. (2000). The transcription factor snail controls epithelial-Mesenchymal transitions by repressing E-cadherin expression. *Nat. Cell Biol.* **2**, 76-83.
- Catala, M., Teillet, M. A. and Le Douarin, N. M. (1995). Organization and development of the tail bud analyzed with the quail-chick chimaera system. *Mech. Dev.* **51**, 51-65.
- Chan, B. W., Chan, K. S., Koide, T., Yeung, S. M., Leung, M. B., Copp, A. J., Loeken, M. R., Shiroishi, T. and Shum, A. S. (2002). Maternal diabetes increases the risk of caudal regression caused by retinoic acid. *Diabetes* **51**, 2811-2816.
- Chapman, S. C., Schubert, F. R., Schoenwolf, G. C. and Lumsden, A. (2002). Analysis of spatial and temporal gene expression patterns in blastula and gastrula stage chick embryos. *Dev. Biol.* **245**, 187-199.

- Chuai, M., Zeng, W., Yang, X., Boychenko, V., Glazier, J. A. and Weijer, C. J. (2006). Cell movement during chick primitive streak formation. *Dev. Biol.* **296**, 137-149.
- Cohn, M. J. and Tickle, C. (1996). Limbs: a model for pattern formation within the vertebrate body plan. *Trends Genet.* **12**, 253-257.
- Davies, J., Chagen, E. and Nance, W. E. (1970). Symmelia in one of monozygotic twins. *Teratology* **4**, 367-378.
- de Santa Barbara, P. and Roberts, D. J. (2002). Tail gut endoderm and gut/genitourinary/tail development: a new tissue-specific role for Hox13. *Development* **129**, 551-561.
- Duhamel, B. (1961). From the mermaid to anal imperforation: the syndrome of caudal regression. *Arch. Dis. Child.* **36**, 152-155.
- Eyal-Giladi, H. (1991). The early embryonic development of the chick, an epigenetic process. *Crit. Rev. Poult. Biol.* **3**, 143-166.
- Faure, S., de Santa Barbara, P., Roberts, D. J. and Whitman, M. (2002). Endogenous patterns of BMP signaling during early chick development. *Dev. Biol.* **244**, 44-65.
- Fujiwara, H., Hayashi, Y., Sanzen, N., Kobayashi, R., Weber, C., Emoto, T., Futaki, S., Niwa, H., Murray, P., Edgar, D. et al. (2007). Regulation of mesodermal differentiation of mouse embryonic stem cell by basement membranes. *J. Biol. Chem.* **282**, 29701-29711.
- Globus, M. and Vethamany Globus, S. (1976). An in vitro analogue of early chick limb bud outgrowth. *Differentiation* **6**, 91-96.
- Gofflot, F., Hall, M. and Morriss Kay, G. M. (1997). Genetic patterning of the developing mouse tail at the time of posterior neuropore closure. *Dev. Dyn.* **210**, 431-445.
- Goldman, D. C., Martin, G. R. and Tam, P. P. (2000). Fate and function of the ventral ectodermal ridge during mouse tail development. *Development* **127**, 2113-2123.
- Greco, T. L., Takada, S., Newhouse, M. M., McMahon, J. A., McMahon, A. P. and Camper, S. A. (1996). Analysis of the vestigial tail mutation demonstrates that Wnt-3a gene dosage regulates mouse axial development. *Genes Dev.* **10**, 313-324.
- Gruneberg, H. (1956). A ventral ectodermal ridge of the tail in mouse embryos. *Nature* **177**, 787-788.
- Hamburger, V. and Hamilton, H. (1951). A series of normal stages in the development of the chick embryo. *J. Morphol.* **88**, 49-92.
- Haraguchi, R., Suzuki, K., Murakami, R., Sakai, M., Kamikawa, M., Kengaku, M., Sekine, K., Kawano, H., Kato, S., Ueno, N. et al. (2000). Molecular analysis of external genitalia formation: the role of fibroblast growth factor (Fgf) genes during genital tubercle formation. *Development* **127**, 2471-2479.
- Harrison, F., Callebaut, M. and Vakaet, L. (1991). Features of polygression and primitive streak ingression through the basal lamina in the chicken blastoderm. *Anat. Rec.* **229**, 369-383.
- Iimura, T. and Pourquie, O. (2006). Collinear activation of Hoxb genes during gastrulation is linked to mesoderm cell ingression. *Nature* **442**, 568-571.
- Jones, C. M., Lyons, K. M. and Hogan, B. L. (1991). Involvement of Bone Morphogenetic Protein-4 (BMP-4) and Vgr-1 in morphogenesis and neurogenesis in the mouse. *Development* **111**, 531-542.
- Knezevic, V., De Santo, R. and Mackem, S. (1998). Continuing organizer function during chick tail development. *Development* **125**, 1791-1801.
- Komatsu, Y., Scott, G., Nagy, A., Kaartinen, V. and Mishina, Y. (2007). BMP type I receptor ALK2 is essential for proper patterning at late gastrulation during mouse embryogenesis. *Dev. Dyn.* **236**, 512-517.
- Lawson, A. and Schoenwolf, G. C. (2001). Cell populations and morphogenetic movements underlying formation of the avian primitive streak and organizer. *Genesis* **29**, 188-195.
- Lepilina, A., Coon, A. N., Kikuchi, K., Holdway, J. E., Roberts, R. W., Burns, C. G. and Poss, K. D. (2006). A dynamic epicardial injury response supports progenitor cell activity during zebrafish heart regeneration. *Cell* **127**, 607-619.
- Li, Y., Litingtung, Y., Ten Dijke, P. and Chiang, C. (2007). Aberrant Bmp signaling and notochord delamination in the pathogenesis of esophageal atresia. *Dev. Dyn.* **236**, 746-754.
- Liem, K. F., Jr, Tremml, G., Roelink, H. and Jessell, T. M. (1995). Dorsal differentiation of neural plate cells induced by BMP-mediated signals from epidermal ectoderm. *Cell* **82**, 969-979.
- Liu, J. P. and Jessell, T. M. (1998). A role for rhoB in the delamination of neural crest cells from the dorsal neural tube. *Development* **125**, 5055-5067.
- McMahon, A., Ingham, P. W. and Tabin, C. J. (2003). Developmental roles and clinical significance of Hedgehog signaling. *Curr. Top. Dev. Biol.* **53**, 1-113.
- McMahon, J. A., Takada, S., Zimmerman, L. B., Fan, C. M., Harland, R. M. and McMahon, A. P. (1998). Noggin-mediated antagonism of BMP signaling is required for growth and patterning of the neural tube and somite. *Genes Dev.* **12**, 1438-1452.
- Miller, S. A. and Briglin, A. (1996). Apoptosis removes chick embryo tail gut and remnant of the primitive streak. *Dev. Dyn.* **206**, 212-218.
- Mills, C. L. and Bellairs, R. (1989). Mitosis and cell death in the tail of the chick embryo. *Anat. Embryol.* **180**, 301-308.
- Mishina, Y., Suzuki, A., Ueno, N. and Behringer, R. R. (1995). Bmpr encodes a type I bone morphogenetic protein receptor that is essential for gastrulation during mouse embryogenesis. *Genes Dev.* **9**, 3027-3037.
- Muller, F. and O'Rahilly, R. (2004). The primitive streak, the caudal eminence and related structures in staged human embryos. *Cells Tissues Organs* **177**, 2-20.
- Nakashima, A., Katagiri, T. and Tamura, M. (2005). Cross-talk between Wnt and bone morphogenetic protein 2 (BMP-2) signaling in differentiation pathway of C2C12 myoblasts. *J. Biol. Chem.* **280**, 37660-37668.
- Ohta, K., Lupo, G., Kuriyama, S., Keynes, R., Holt, C. E., Harris, W. A., Tanaka, H. and Ohnuma, S. (2004). Tsukushi functions as an organizer inducer by inhibition of BMP activity in cooperation with chordin. *Dev. Cell* **7**, 347-358.
- Ohta, S., Suzuki, K., Tachibana, K. and Yamada, G. (2003). Microbubble-enhanced sonoporation: efficient gene transduction technique for chick embryos. *Genesis* **37**, 91-101.
- Ohta, S., Ogino, Y., Suzuki, K., Kaminura, M., Tachibana, K. and Tamada, G. (2007). Sonoporation: an efficient technique for the introduction of genes into chick embryos. In *Gene Transfer: Delivery and Expression of DNA and RNA* (ed. T. Friedmann and J. Rossi), pp. 711-716. Cold Spring Harbor: Cold Spring Harbor Laboratory Press.
- Peinado, H., Quintanilla, M. and Cano, A. (2003). Transforming growth factor beta-1 induces snail transcription factor in epithelial cell lines: mechanisms for epithelial Mesenchymal transitions. *J. Biol. Chem.* **278**, 21113-21123.
- Pyati, U. J., Cooper, M. S., Davidson, A. J., Nechiporuk, A. and Kimelman, D. (2006). Sustained Bmp signaling is essential for cloaca development in zebrafish. *Development* **133**, 2275-2284.
- Reiter, R. S. and Solursh, M. (1982). Mitogenic property of the apical ectodermal ridge. *Dev. Biol.* **93**, 28-35.
- Sakai, D., Tanaka, Y., Endo, Y., Osumi, N., Okamoto, H. and Wakamatsu, Y. (2005). Regulation of Slug transcription in embryonic ectoderm by beta-catenin-Lef/Tcf and BMP-Smad signaling. *Dev. Growth Differ.* **16**, 471-482.
- Schoenwolf, G. C. (1979a). Histological and ultrastructural observations of tail bud formation in the chick embryo. *Anat. Rec.* **193**, 131-147.
- Schoenwolf, G. C. (1979b). Observations on closure of the neuropores in the chick embryo. *Am. J. Anat.* **155**, 445-465.
- Schoenwolf, G. C. (1981). Morphogenetic processes involved in the remodeling of the tail region of the chick embryo. *Anat. Embryol.* **162**, 183-197.
- Shook, D. and Keller, R. (2003). Mechanisms, mechanics and function of epithelial-Mesenchymal transitions in early development. *Mech. Dev.* **120**, 1351-1383.
- Song, W., Jackson, K. and McGuire, P. G. (2000). Degradation of type IV collagen by matrix metalloproteinases is an important step in the epithelial-Mesenchymal transformation of the endocardial cushions. *Dev. Biol.* **227**, 606-617.
- Stern, C. D. (1990). The marginal zone and its contribution to the hypoblast and primitive streak of the chick embryo. *Development* **109**, 667-682.
- Suzuki, K., Bachiller, D., Chen, Y. P., Kamikawa, M., Ogi, H., Haraguchi, R., Ogino, Y., Minami, Y., Mishina, Y., Ahn, K. et al. (2003). Regulation of outgrowth and apoptosis for the terminal appendage: external genitalia development by concerted actions of BMP signaling [corrected]. *Development* **130**, 6209-6220.
- Tachibana, K. and Tachibana, S. (1995). Albumin microbubble echo-contrast material as an enhancer for ultrasound accelerated thrombolysis. *Circulation* **92**, 1148-1150.
- Takada, S., Stark, K. L., Shea, M. J., Vassileva, G., McMahon, J. A. and McMahon, A. P. (1994). Wnt-3a regulates somite and tailbud formation in the mouse embryo. *Genes Dev.* **8**, 174-189.
- Tam, P. P. and Beddington, R. S. (1987). The formation of mesodermal tissues in the mouse embryo during gastrulation and early organogenesis. *Development* **99**, 109-126.
- Tam, P. P. and Tan, S. S. (1992). The somitogenic potential of cells in the primitive streak and the tail bud of the organogenesis-stage mouse embryo. *Development* **115**, 703-715.
- Thiery, J. P. (2002). Epithelial-Mesenchymal transitions in tumour progression. *Nat. Rev. Cancer* **2**, 442-454.
- Tucker, A. S. and Slack, J. M. (2004). Independent induction and formation of the dorsal and ventral fins in *Xenopus laevis*. *Dev. Dyn.* **230**, 461-467.
- Vakaet, L. (1984). The initiation of gastrula ingression in the chick blastoderm. *Am. Zool.* **24**, 555-562.
- Wang, S., de Caestecker, M., Kopp, J., Mitu, G., Lapage, J. and Hirschberg, R. (2006). Renal bone morphogenetic protein-7 protects against diabetic nephropathy. *J. Am. Soc. Nephrol.* **17**, 2504-2512.
- Wilson, V. and Beddington, R. S. (1996). Cell fate and morphogenetic movement in the late mouse primitive streak. *Mech. Dev.* **55**, 79-89.
- Winnier, G., Blessing, M., Labosky, P. A. and Hogan, B. L. (1995). Bone morphogenetic protein-4 is required for mesoderm formation and patterning in the mouse. *Genes Dev.* **9**, 2105-2116.
- Zakin, L., Reversade, B., Kuroda, H., Lyons, K. M. and De Robertis, E. M. (2005). Sirenomelia in Bmp7 and Tsg compound mutant mice: requirement for Bmp signaling in the development of ventral posterior mesoderm. *Development* **132**, 2489-2499.
- Zhang, H. and Bradley, A. (1996). Mice deficient for BMP2 are nonviable and have defects in amnion/chorion and cardiac development. *Development* **122**, 2977-2986.